POLITECNICO DI TORINO
Repository ISTITUZIONALE

Multi Scale Numerical Modelling Related to Hydrofracking for Deep Geothermal Energy Exploitation

Original
Multi Scale Numerical Modelling Related to Hydrofracking for Deep Geothermal Energy Exploitation / Insana, A., Barla, M., Elmo, D.. - In: PROCEDIA ENGINEERING. - ISSN 1877-7058. - ELETTRONICO. - 158:(2016), pp. 314-319. (VI Italian Conference of Researchers in Geotechnical Engineering (CNRIG2016) Bologna (IT) 22-23 Settembre 2016) [10.1016/j.proeng.2016.08.448].

Availability:
This version is available at: 11583/2650270 since: 2025-01-02T10:57:56Z

Publisher:
Elsevier

Published
DOI:10.1016/j.proeng.2016.08.448

Terms of use:

This article is made available under terms and conditions as specified in the corresponding bibliographic description in the repository

Publisher copyright

(Article begins on next page)

29 November 2026

Available online at www.sciencedirect.com

ScienceDirect

Procedia Engineering 158 (2016) 314 – 319

Procedia Engineering

www.elsevier.com/locate/procedia

VI ITALIAN CONFERENCE OF RESEARCHERS IN GEOTECHNICAL ENGINEERING – Geotechnical Engineering in Multidisciplinary Research: from Microscale to Regional Scale, CNRIG2016

Multi scale numerical modelling related to hydrofracking for deep geothermal energy exploitation

Alessandra Insana[a], Marco Barla[a,*], Davide Elmo[b]

[a]*Dipartimento di Ingegneria Strutturale, Edile e Geotecnica, Politecnico di Torino, Corso Duca degli Abruzzi 24, Torino 10129, Italy*
[b]*Norman B. Keevil Institute of Mining Engineering, University of British Columbia, 6350 Stores Road, Vancouver BC V6T 1Z4, Canada*

Abstract

Prediction of fracture propagation through rock masses is investigated in this paper by adopting the Distinct Element Method (DEM) and the Voronoi tessellation. A microstructure-based model was created. Microparameters governing Voronoi sub-blocks contacts behaviour were calibrated against laboratory tests results for different rocks. An upscaling procedure is proposed to build reliable and representative numerical models at in situ scale to study fracture propagation for deep geothermal wells.
© 2016 The Authors. Published by Elsevier Ltd. This is an open access article under the CC BY-NC-ND license (http://creativecommons.org/licenses/by-nc-nd/4.0/).
Peer-review under the responsibility of the organizing and scientific committees of CNRIG2016

Keywords: Fracture process; Voronoi tessellation; geothermal wells

1. Introduction

Enhanced Geothermal System (EGS) are engineered reservoirs created to extract heat from economically improductive geothermal resources, typically known as Hot Dry Rock (HDR). An EGS uses drilling, fracturing and injection to provide fluid and permeability in areas that have hot but dry underground rock [1]. Heat is the only component that needs be natural. Insufficient permeability is remedied by artificial means such as hydraulic fracturing, by means of which high-pressure water is injected from the surface through wells into a body of deep, hot, compact rock to enlarge preexisting sealed fractures or to create new ones. Water permeates these fracture

* Corresponding author. Tel.: +39-011-090-4824.
E-mail address: marco.barla@polito.it

1877-7058 © 2016 The Authors. Published by Elsevier Ltd. This is an open access article under the CC BY-NC-ND license (http://creativecommons.org/licenses/by-nc-nd/4.0/).
Peer-review under the responsibility of the organizing and scientific committees of CNRIG2016
doi:10.1016/j.proeng.2016.08.448

system, flows along permeable pathways, extracting heat from the surrounding rock. This reservoir is later penetrated by a second well, which is used to extract the heated water. Upon leaving the plant, the fluid is returned to the reservoir through injection wells to complete the circulation loop.

Despite hydraulic fracturing technology having been used for more than 30 years in the context of energy exploitation, underground formations represent a complex system of variables (both rock and well properties) that make fracturing processes a not fully understood problem that requires further investigation [2-4]. Prediction of the effectiveness of the fracturing process can be investigated by numerical simulations [5-8]. For problems in which large-scale phenomena (e.g. rock slides or reservoir stimulation) are strongly influenced by processes occurring at much smaller scales (e.g. fracture initiation and propagation), it is not practical to generate comprehensive simulations that include an explicit representation of the fracturing processes over a wide range of scales. To address this problem, numerical methods may be used with a multi-scale approach combining multiple models defined at fundamentally different length scales within the same overall spatial domain [2, 9-13]. For example, a small-scale model with high resolution can be utilized in a fraction of the overall domain and linked to a large-scale model with coarse resolution over the remainder of the overall domain, providing necessary efficiency of characterization and computation that will render solution of these problems practical.

This paper will focus on the simulation of hydrofracking processes for the creation of an EGS system by a multi-scale approach. The Voronoi tessellation [14] and the Distinct Element Method (DEM) [15] will be used to reproduce rock behavior at the laboratory scale. An upscale procedure will be presented to finally model the fracturing process at the site scale. The theoretical but realistic case study of a man-made geothermal field concerning a granitic rock mass will be discussed.

2. Multi scale modelling approach

The multi scale modelling approach was implemented with the DEM and the UDEC software [16]. Voronoi tessellation was used to generate the synthetic rock material. The Voronoi tessellation is a special joint generator that creates randomly sized polygonal or triangular (option Trigon) blocks. The grain boundaries in the poly-crystal structure produced by Voronoi tessellation can be used to represent flaws in intact rock and therefore allow for simulation of crack damage development through initiation and propagation of fractures along grain boundaries [16].

The parameters governing the behavior of Voronoi elements have to be calibrated and verified against reliable laboratory experiments. To this extent, uniaxial compression tests (UCS) and indirect tensile strength tests were simulated for a number of rock types. Synthetic specimens of 50 mm in diameter and 100 mm in height were prepared (Fig. 1a), in which a Voronoi edge of 3 mm was chosen. Five different rocks were considered: Plaster of Paris [17], Transjurane sandstone [18], Tagikistan siltstone, Augig granite [18] and Barre granite, allowing to assess the differences in the calibration of the Voronoi sub-blocks contacts microparameters.

The constitutive model of the sub-blocks is assumed as isotropic elastic, while an elasto-plastic behavior with softening and a Mohr-Coulomb failure criterion is assigned to the Voronoi contacts. A constant loading rate of 0.001 m/s was applied to the top and bottom platens to simulate uniaxial loading tests. The loading rate was found to be a good compromise between computational time and precision of the results in previous studies.

The calibration process was performed by means of a trial-and-error procedure where the material macro properties are modified by two factors S and R defined as follows:

$$k_{n,trial} = S \cdot k_{n,mat} \qquad k_{s,trial} = k_{n,trial} / 2 \tag{1}$$

$$c_{trial} = R \cdot c_{mat} \qquad tg\Phi_{trial} = R \cdot tg\Phi_{mat} \qquad \sigma_{t,trial} = R \cdot \sigma_{t,mat} \tag{2}$$

where k_n and k_s are the normal and shear stiffnesses, c is the cohesion, Φ the friction angle and σ_t the tensile strength.

At first, R is kept constant and S is gradually increased in order to match the deformability measured during triaxial laboratory tests. Then, the calibrated S value is kept constant and R is modified to match the proper strength. Table 1 shows the results of the calibration process.

Table 1. Strength and deformability parameters from numerical analysis after calibration.

	R	S	σ_{ci} [MPa]	E [MPa]	σ_t [MPa]
Plaster of Paris	1.29	1.25	4.83	4450	0.37
Transjurane sandstone	1.29	1.25	39.18	12321	1.60
Tagikistan siltstone	1.29	3	75.67	12434	4.05
Augig granite	1.33	3	113.55	25568	6.86
Barre granite	1.2	1.25	94.22	39436	5.85

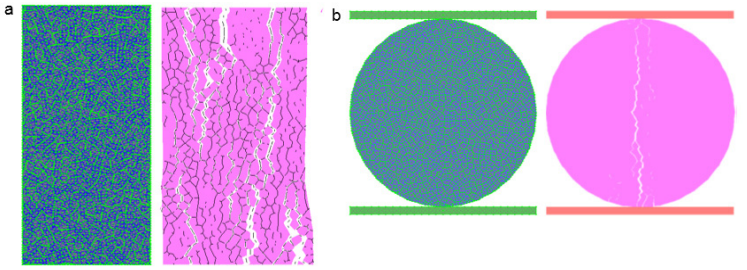

Fig. 1. UCS (a) and indirect tensile strength (b) test specimens before and at the end of the test for Barre granite.

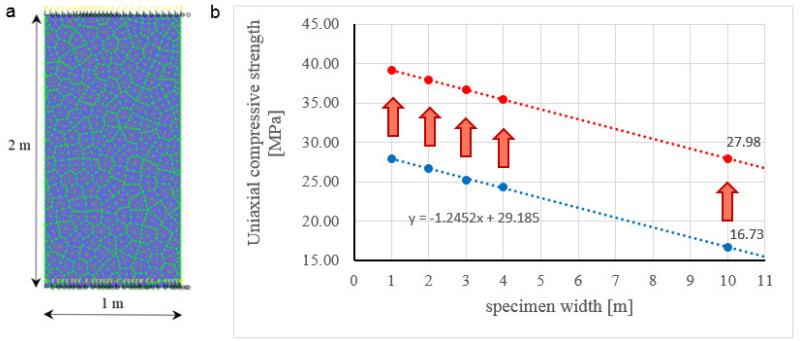

Fig. 2. (a) 1 x 2 m sample with a Voronoi size of 10 cm; (b) Calibration procedure at the site scale.

Figure 1a highlights the typical axial splitting behavior [19-20] at the end of the simulation. The calibrated parameters were then used to model indirect tensile strength tests (Fig. 1b). The modelled values of tensile strength were found to be in good agreement with the experimental data. It was found that the computational time for the analyses was highly influenced by the size of the Voronoi element; for a model intended to simulate the in situ behavior of a rock mass (scale of tens of meters), using an element size of 3 mm would make the simulation computationally impractical. For the current analysis, it was decided to use a Voronoi size of 10 cm, which in the authors' opinion represents a good compromise between accuracy of modelled results and computational time.

With the new Voronoi edge length, new values of R and S were calibrated over a 1 x 2 m sample (Fig. 2a) to reproduce directly rock mass deformability and strength. The influence of the scale was then investigated by creating UCS specimens at different scales (width = 1 m, 2 m, 3 m, 4 m) adopting the same Voronoi edge length and microparameters. This has allowed to derive a linear reduction of the unconfined strength with increasing scale. The linear interpolation shown in Figure 2b was then used to predict the strength at the scale of interest (10 x 20 m for the application described in section 3). To this extent, it was necessary to shift the line upwards by increasing the R factor by trial-and error, in order to match the required field strength. Since strength is only affected by the parameter R, S is kept constant. This procedure has allowed preparing site scale models discretized with Voronoi elements that would yield a reasonable mechanical behavior.

4. Simulation of the hydrofracking process

The simulation of the hydrofracking process at the site scale was performed with reference to the case study of a theoretical man-made geothermal field. A new DEM model was built to reproduce two vertical circular boreholes with a diameter of 50 cm, and 5 m apart, drilled in a granitic rock mass. The model simulates the excavation process of the boreholes by removal of the elements and the application of an internal pressure due to bentonite mud. Subsequently, an increase of the internal pressure simulates the hydrofracking of the rock mass at a depth of 4 km, with the aim of creating a system of fractures. The properties of the rock mass are given in Table 2.

Table 2. Barre granite geological and mechanical properties (intact rock and rock mass).

Property	Symbol	Value	Property	Symbol	Value
Density [kg/m3]	ρ	2640	Cohesion [MPa]	c	7.3
Poisson's ratio [-]	ν	0.3	Rock mass tensile strength [MPa]	σ_t	0.08
Rock mass Young's modulus [GPa]	E	40	Rock mass UCS strength [MPa]	σ_c	28.0
Friction angle [°]	Φ	34.6			

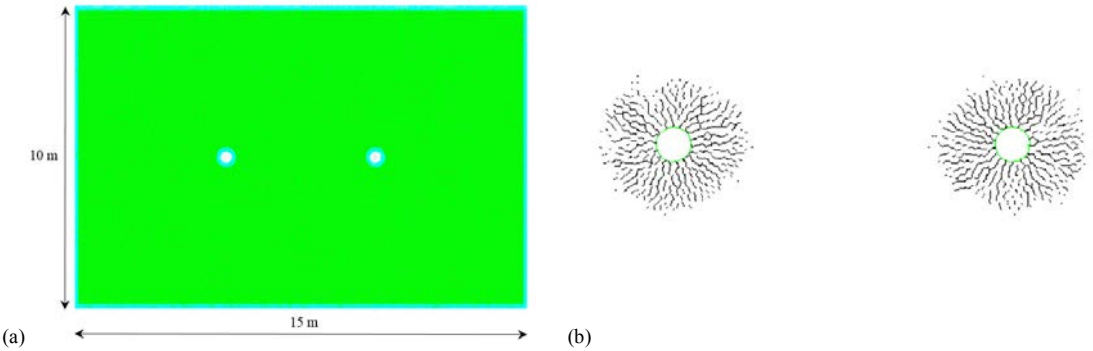

Fig. 3. (a) Geometry of the 10 x 15 m model, with 5 m distance between the holes and (b) gradual creation of a plastic zone around the boreholes.

An isotropic in situ stress state is assumed for the 2D section, therefore both the horizontal stresses are assumed equal to 105.6 MPa. The size of the Voronoi (10 cm) is assumed based on the conclusions of section 2. As the calculation speed is essentially a linear function of the number of blocks used in the model [16], the model size was limited to 10 x 15 m in order to reduce the size of the discretized domain and thus limiting the required computational time (Fig. 3a). In the field, the bentonitic mud is injected starting from a certain depth, with the purpose to remove cuttings, help prevent blowouts and stabilize the excavation. In the model, mud injection was simulated starting from 500 m depth. The internal pressure to be applied, reproducing mud pressure at a depth of 4 km, was therefore 35.6 MPa.

The simulation is carried out by means of a sequence of stages. During model initialization, each element is assigned the in-situ stress state and stress boundary conditions are applied. Once the drilling of the two boreholes is completed, hydraulic pressure inside the boreholes is gradually increased starting from 35.6 MPa up to the value needed to reach the continuity of the fracture network (50 MPa, 100 MPa, 150 MPa…). This causes the opening and propagation of a cracking system within the rock mass.

Simple application of an internal pressure inside the borehole would generate a concentric plastic zone around the two boreholes. Figure 3b shows an example of the fracture pattern which results from the application of a 1000 MPa internal pressure. This clearly does not appropriately reproduce the mechanisms occurring in the field, where the fluid would permeate the fractures as those are progressively extending. To perform a more realistic simulation of the development of the fracture process in the rock mass, a new procedure was written by taking advantage of the FISH built-in programming language available in the UDEC software. The FISH function is built to simulate permeation of the fluid into the fractures as those are being formed. Figure 4 illustrates schematically how the FISH function operates. First, a pressure *p* is applied to the boreholes boundary (a). By increasing the pressure, at a certain

point, fractures start to occur on the boundary (Fig. 4b shows in red an example of first fractures created). At this point, every domain (void or space between blocks defined by two or more contacts) within the model is scanned by the FISH function, excluding the domain indices corresponding to the boreholes. Each domain contacts indices are detected and the contacts coordinates are saved. The orientation of the contacts is computed geometrically, together with the horizontal and vertical components of p. If the normal displacement is positive, the FISH function recognizes a joint where failure occurred and assigns a normal pressure equal to p to the whole domain including that contact. In this way, the pressure is also applied into the newly created fractures (c). This causes fractures to propagate. For every pressure increase, the FISH function is run as long as new fractures are created, and then pressure is increased up to the value required in the next step. For example, at the beginning of the computation process, when internal pressure is lower (50 MPa to 100 MPa), the FISH function was run twice for 50000 steps because the propagation and expansion of fractures was found to be completed in a relatively short period of time. On the contrary, once the internal pressure reaches 300 MPa, four stages made up of 50000 steps each are required. Applying 350 MPa on the boreholes boundary, the FISH function was run 42 times requiring about 3-4 hours for each stage. The overall computational time was about two weeks.

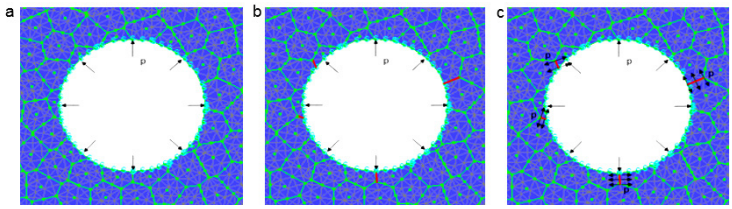

Fig. 4. FISH function mode of operation.

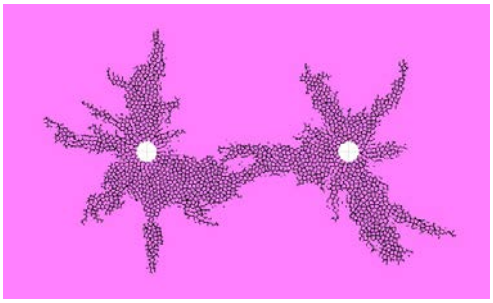

Fig. 5. Fractures network corresponding to the final pressure of 350 MPa.

The fracture pattern which results from the computation is shown in Figure 5. Continuity of fractures between the two boreholes is obtained by the application of an internal pressure of 350 MPa. As the initial stress state is isotropic, fractures propagate in different directions even if some of these are more evident. Once fractures expanding from each borehole approach the central zone in between the boreholes, they start to interact and thus generating a network of connecting fractures within the two boreholes. Although no in situ data are available (pressure value or fracture pattern), these results would appear to be very realistic.

4. Conclusions

The modelling work presented in this paper allows to draw the following conclusions:

- Creating an assembly of distinct elements with the Voronoi tessellation allows to build synthetic rock specimens and realistically reproduce rock fragmentation experienced during laboratory testing.

- Microparameters controlling deformability and strength of the contact between Voronoi elements need to be calibrated against laboratory data. Two factors S and R, related to stiffness and strength respectively, were introduced to simplify the calibration process.
- Strength of synthetic specimens is shown to be affected by scale effect: by keeping constant the Voronoi edge length, the strength decreases linearly with the size of the specimen.
- The computational time is highly influenced by the size of the Voronoi element. For model intended to simulate the in situ behavior of a rock mass, element size of less than 10 cm are practically inapplicable.
- A multi-scale numerical approach was developed to simulate rock hydrofracking in EGS systems by using Voronoi tessellation and the distinct element method. Unconfined compressive strength of specimens of different sizes was determined. The linear trend was extended to determine factors S and R pertinent to the in situ scale.
- To reproduce the progressive fracturing of the rock mass and the creation of fracture patterns, a FISH function was written to allow detecting new fractures and apply normal pressure within them.

Although the result of the computation show a very realistic fracture pattern, some caution need to be adopted in analyzing results and additional improvements are needed. The polygonal Voronoi geometry plays a key role in the generation and extension of cracks. The result is therefore mesh dependent unless very small elements are used, which however is impractical. Moreover, the present version of the FISH function is not able to distinguish between communicating and not communicating fractures. This may slightly affect the resulting fracture pattern. These aspects can be dealt with by testing the Voronoi Trigon, which allows for triangular elements to be created, and by improving the FISH function.

References

[1] I. Johnston, G. Narsilio, S. Colls, Emerging geothermal energy technologies, KSCE J. Civ. Eng. 14(4) (2011) 643-653.
[2] Y. Sheng, M. Susani, D. Ingham, M. Pourkashanian, Recent developments in multiscale and multiphase modelling of hydraulic fracturing process, Mathematical Problems in Engineering, Hindawi Publishing Corporation, Article ID 729672 (2015) 1-15.
[3] E. Ghazvinian, M.S. Diederichs, R. Quey, 3D random Voronoi grainbased models for simulation of brittle rock damage and fabric-guided microfracturing, J. of Rock Mech. Geotech. Eng. 6 (2014) 506-521.
[4] M. Barla, F. Antolini, Combined Finite-Discrete numerical modeling of rock spalling in tunnels, 14th International conference of the International Association for Computer Methods and Advances in Geomechanics, Kyoto, 21-24 September (2014) 1595-1600.
[5] M. Wangen, Finite element modeling of hydraulic fracturing on a reservoir scale in 2D, J. Pet. Sci. Eng. 77 (2011) 274-285.
[6] A. Al-Busaidi, J.F. Hazzard, R.P. Young, Distinct element modeling of hydraulically fractured Lac du Bonnet granite, J. Geophys. Res. 110 (2005) B06302.
[7] S. Deng, R. Podgorney, H. Huang, Discrete element modeling of rock deformation, fracture network development and permeability evolution under hydraulic stimulation, Proceedings of the 36th Workshop on Geothermal Reservoir Engineering, Stanford University, 2011.
[8] Y. Wang, D. Adhikary, Hydraulic fracture simulation based on coupled discrete element method and lattice boltzmann method, Proceedings of the World Geothermal Congress, Melbourne, Australia, 2015.
[9] F. Gao, D. Stead, The application of a modified Voronoi logic to brittle fracture modelling at the laboratory and field scale, Int. J. Rock Mech. Min. Sci. 68 (2014) 1–14.
[10] M. Sousani, Modeling of hydraulic fracturing in rocks: a multiscale and fluid-solid coupling approach, PhD thesis, Univ. of Leeds, 2015.
[11] M. Barla, M. Camusso, A method to design microtunnelling installations in the Torino randomly cemented alluvial soil, Tunnelling and Underground Space Technology 33 (2013) 73-81.
[12] M. Barla, G. Barla, Torino subsoil characterisation by combining site investigations and numerical modelling, Geomechanik und Tunnelbau, 5(3) (2012).
[13] M. Camusso, M. Barla, Microparameters calibration for loose and cemented soil when using particle methods, Int. J. Geomech. 9(5) (2009) 217-230.
[14] L.J. Lorig, P.A. Cundall, Modelling of reinforced concrete using the Distinct Element Method, Proc. SEM/RILEM Int. Conf. on Fracture of Concrete and Rock, SEM, Bethel Connecticut (1987) 459-471.
[15] P.A. Cundall, O.D.L. Strack, A discrete numerical model for granular assemblies, Géotechnique 29(1) (1979) 47-65.
[16] A.K. Alzo'ubi, Modeling of rocks under direct shear loading by using Discrete Element Method, J. of Eng. & App. Sci. 4(2) (2012) 5-20.
[17] T. Kazerani, J. Zhao, Micromechanical parameters in bonded particle method for modelling of brittle material failure, International Journal for Numerical and Analytical Methods in Geomechanics 34 (2010) 1877-1895.
[18] O.K. Mahabadi, A. Lisjak, G. Grasselli, Numerical modelling of a triaxial test of homogeneous rocks using the combined finite-discrete element method, Proceedings of the European rock mechanics symposium, Lausanne, Switzerland, 2010.
[19] P. Hamdi, D. Stead, D. Elmo, Damage characterization during laboratory strength testing: a 3D-finite-discrete element approach, Computers and Geotechnics 60 (2014) 33–46.